JOURNAL OF MATERIALS SCIENCE 30 (1995) 196–200

# Thermodynamic analysis of irradiation-induced amorphization of intermetallic particles in Zircaloy

C. RODRÍGUEZ, R. H. DE TENDLER*
*Gerencia de Desarrollo, Comisión Nacional de Energía Atómica, Avda. del Libertador 8250, 1429 Buenos Aires, Argentina*

L. J. GALLEGO
*Dpto. de Física de la Materia Condensada, Facultad de Física, Universidad de Santiago de Compostela, Santiago de Compostela, Spain*

J. A. ALONSO
*Dpto. de Física Teórica, Facultad de Ciencias, Universidad de Valladolid, Valladolid, Spain*

The intermetallic precipitate particles $Zr_2(Ni, Fe)$ in Zircaloy-2 and $Zr(Cr, Fe)_2$ in Zircaloy-4, dissolve and amorphize under irradiation. Pursuing a previous analysis by Motta and Lemaignan, we have studied those effects on the basis of the metastable free-energy diagram of the reference system Zr–Fe (calculated using Miedema's model) and considering some aspects of the modification of this free-energy diagram by irradiation. We then can explain why both phases $Zr_2(Ni, Fe)$ and $Zr(Cr, Fe)_2$ can be amorphized at low temperatures (below 350 K) without composition changes if sufficient energy can be accumulated by irradiation-produced defects and chemical disorder, and also that at intermediate temperatures (about 580 K) a driving force exists for particle amorphization at the matrix–particle interface for $Zr(Cr, Fe)_2$ but not for $Zr(Ni, Fe)_2$.

## 1. Introduction

In the amorphization of metallic alloys by irradiation, two situations are commonly encountered. In one, amorphization occurs at the interface of metals or alloys in contact, and is mainly attributed to ion mixing. In the other, ordered intermetallic phases can be homogeneously amorphized by internal accumulation of free energy due to chemical long-range disorder or to the buildup of simple irradiation defects or defect complexes [1, 2]. Departures from stoichiometry [1] and irradiation-produced defects [2] are believed to play key roles in the destabilization of the compound.

Zirconium-based alloys such as Zircaloy-2 and 4 are used in nuclear reactors. These alloys contain small amounts of tin, iron, chromium and nickel and present a number of precipitate intermetallic particles rich in those elements [3–5]. A variety of intermetallic phases, structures and compositions have been reported to occur simultaneously. Nevertheless, the phases most frequently found are hexagonal close-packed $Zr(Cr, Fe)_2$ and body-centred tetragonal $Zr_2(Ni, Fe)$ in Zircaloy-4 and Zircaloy-2, respectively. Both kinds of particles have been reported to dissolve and amorphize under irradiation.

At low temperatures (below 350 K), both kinds of particles amorphize under electron, heavy-ion and neutron irradiation [6–8]. Dissolution of both particles was also reported to occur by neutron irradiation [6] but not by electron irradiation [8]. At intermediate temperatures (about 580 K), irradiation dissolution of $Zr_2(Ni, Fe)$ and amorphization of $Zr(Cr, Fe)_2$ occurs. Amorphization from the periphery inwards to the centre of the $Zr(Cr, Fe)_2$ intermetallic, with iron depletion in the amorphous layer, was reported to occur by neutron irradiation [6, 9–14]. At high temperatures (above 640 K), both kinds of particles remain crystalline and dissolve [5, 8, 10, 12, 15]. Complete dissolution of $Zr(Cr, Fe)_2$ without reprecipitation was reported [10], although reprecipitation of the former particles and new ones has also been observed [12, 15].

Two types of arguments have been used to describe these effects. In one, the destabilizing effect of irradiation-induced point defects fluxes has been raised, while in the other an irradiation-modified thermodynamic local phase equilibrium was qualitatively described [13]. In the present work, we proceed along the lines proposed by Motta and Lemaignan [13] and extend their qualitative analysis by calculating the free

* Author to whom all correspondence should be addressed.



0022–2461 

energies of some stable and metastable phases for the reference model system Zr–Fe by means of the Miedema model [16–23]. Plausible modifications of the free-energy diagram by irradiation will be considered to describe the new local "equilibrium conditions". With this simple approach, the different amorphization behaviour of $Zr_2(Ni, Fe)$ and $Zr(Cr, Fe)_2$ can be qualitatively understood.

## 2. Calculation of the metastable free-energy diagram of the Zr–Fe alloy

Our analysis is based on the comparison of the free energies of some stable and metastable phases of the Zr–Fe alloy. Those will be calculated using a semi-empirical theory due to Miedema and co-workers [16–23] and further developed by López *et al.* [24]. As we discuss extensively in Section 3 below, the phases whose free energies are to be compared are the Zr–Fe amorphous alloy, the metastable solid solutions formed between iron and zirconium and the intermetallic compounds $Zr_2Fe$ and $ZrFe_2$.

The enthalpy of formation of a crystalline solid solution of two transition metals consists of three terms

$$\Delta H_s = \Delta H_c + \Delta H_e + \Delta H_{str} \quad (1)$$

The chemical contribution, $\Delta H_c$, is due to the electron redistribution that occurs when different atoms mix together. The elastic contribution, $\Delta H_e$, originates in the size difference between the two types of atoms, and the structural contribution, $\Delta H_{str}$ depends on the crystalline structure and the valencies of the transition metals that form the solid solution.

The chemical contribution has the form

$$\Delta H_c = \Delta H^{amp} x_{Fe}[V_{Fe}(alloy)]^{2/3} f_{FeZr} \quad (2)$$

where $\Delta H^{amp}$ is an amplitude due to the electron redistribution, $x_{Fe}$ and $V_{Fe}$ (alloy) are, respectively, the atomic fraction and the atomic volume of iron in the alloy [16], and $f_{FeZr}$ which accounts for the degree to which iron atoms are surrounded by zirconium atoms as neighbours, is given by the empirical expression

$$f_{FeZr} = (x^s)_{Zr}\{1 + \gamma[(x^s)_{Zr}(x^s)_{Fe}]^2\} \quad (3)$$

$(x^s)_{Zr}$ and $(x^s)_{Fe}$ being the surface-area concentrations of zirconium and iron in the alloy, and $\gamma$ the parameter that specifies the degree of chemical order. $\gamma$ can take values between that corresponding to disordered alloys ($\gamma = 0$), up to the value corresponding to ordered compounds ($\gamma = 8$). To calculate $\Delta H^{amp}$, $f_{FeZr}$ and $V_{Fe}$ (alloy) using the equations of the Miedema model, the following parameters are used, as defined and tabulated elsewhere [16]: electron densities at the boundary of the Wigner–Seitz cells, electronegativities and molar volumes of the pure metals.

The elastic term is calculated as

$$\Delta H_e = x_{Fe}x_{Zr}[x_{Fe}\Delta h_e(Zr \text{ in } Fe) + x_{Zr}\Delta h_e(Fe \text{ in } Zr)] \quad (4)$$

where $\Delta h_e$ is the elastic energy of the solid solution at infinite dilution, which was modelled with the theory of the elasticity for continuum media [18, 25, 26]. To calculate $\Delta h_e$, we have used the shear and the bulk moduli of Fe(b c c) and Zr(h c p) taken from the compilation in [27].

The structural contribution accounts for the fact that there is a systematic variation of the crystal structure as one moves across the transition metal periods, that is, as the number $z$ of valence (s + d) electrons changes. It is then reasonable also that the structure-dependent energies in solid solutions will vary systematically with the average number of valence electrons per atom if the two metals form a common band of d-type states. Consequently, dissolving metal A in host B changes the energy that stabilizes the crystal structure of the matrix. For our case this structural contribution is

$$\Delta H_{str} = E_\sigma(z_{alloy}) - x_{Fe}E_{bcc}(z_{Fe}) - x_{Zr}E_{hcp}(z_{Zr}) \quad (5)$$

where $\sigma$ symbolizes the crystalline structure of the alloy and the reference state is given by the stable crystalline structure of the pure metals at the temperature of interest: b c c Fe and h c p Zr [28]. $E_\sigma(z)$ are functions giving the lattice stabilities for each one of the three main crystalline structures ($\sigma$ = h c p, f c c, b c c) as a function of the valence, $z$, across the transition metal periods. Those stability functions have been calculated by Niessen and Miedema for non-magnetic metals [18] and also for the ferromagnetic state of metals with more than half-filled d bands [23]. $z_{Fe} = 8$ and $z_{Zr} = 4$ are the valencies of the pure metals, and the valence of the alloy is the concentration averaged value

$$z_{alloy} = x_{Fe}z_{Fe} + x_{Zr}z_{Zr} \quad (6)$$

In the present work, $E_\sigma(z)$ has been calculated taking into account ferromagnetic effects [23, 26].

Now, the free energy of formation of the solid solution is given by the equation

$$\Delta G_s = \Delta H_s - T\Delta S_{str} - T\Delta S_{ideal} \quad (7)$$

where $\Delta H_s$ has already been discussed and the entropy of formation is expressed as the sum of two terms. The first one is the ideal entropy of mixing

$$\Delta S_{ideal} = -R[x_{Fe}\ln x_{Fe} + x_{Zr}\ln x_{Zr}] \quad (8)$$

Similar to Equation 5, there is a contribution, $\Delta S_{str}$, to the entropy of formation when the crystal structure, $\sigma$, of the solid solution formed by zirconium and iron is different from those of one or both metals. We approximate $\Delta S_{str}$ as a weighted average of the entropy contributions to the structural transformations of the pure metals

$$\Delta S_{str} = x_{Zr}(S_\sigma - S_{hcp})_{Zr} + x_{Fe}(S_\sigma - S_{bcc})_{Fe} \quad (9)$$

$(S_\sigma - S_{hcp})_{Zr}$ is the entropy change associated with the structural transformation of pure zirconium from the reference structure (h c p) into the $\sigma$ structure. The value of this structural transformation entropy when

$\sigma$ = bcc was taken from [29]. In a similar way, $(S_\sigma - S_{bcc})_{Fe}$ is the entropy change for the structural transformation of iron from the reference bcc structure into the $\sigma$ structure. To represent the free energy of formation of the metastable solid solution phase as a function of concentration, we have chosen the lower envelope of the $(\Delta G_s)_\sigma$ curves ($\sigma$ = hcp and $\sigma$ = bcc) [19, 20].

The free energy of formation, $\Delta G_a$, of the amorphous, or undercooled, alloy with respect to the pure crystalline metals was calculated by adding to the free energy of mixing of the liquid alloy (referred to as the pure liquid metals) the differences in free energy between the undercooled liquid and crystalline phases of the pure elements, $\Delta G_{as}$ [19–21, 24], i.e.

$$\Delta G_a = \Delta H_c - T\Delta S_{ideal} + x_{Fe}(\Delta G_{as})_{Fe} + x_{Zr}(\Delta G_{as})_{Zr} \quad (10)$$

This equation shows that the free energy of mixing is just the sum of the chemical enthalpy of mixing and the ideal entropy of mixing (elastic and structural terms are, of course, absent in $\Delta G_a$) [19, 20]. $\Delta G_{as}$ is well fitted by the Miedema approximation [21]

$$(\Delta G_{as})_i = 0.0035[(T_m)_i - T]\,(\text{kJ mol}^{-1}) \quad (11)$$

where $T_m$ is the melting temperature of the pure metals, $i$ = Fe, Zr and $(T_m - T)$ is the degree of undercooling.

Finally, the free energies of formation of the intermetallic compounds $Zr_2Fe$ and $ZrFe_2$ are just the enthalpies of formation (the chemical term $\Delta H_c$ with $\gamma = 8$) reported elsewhere [22], as we can assume that the entropy of compound formation is negligible [22, 24].

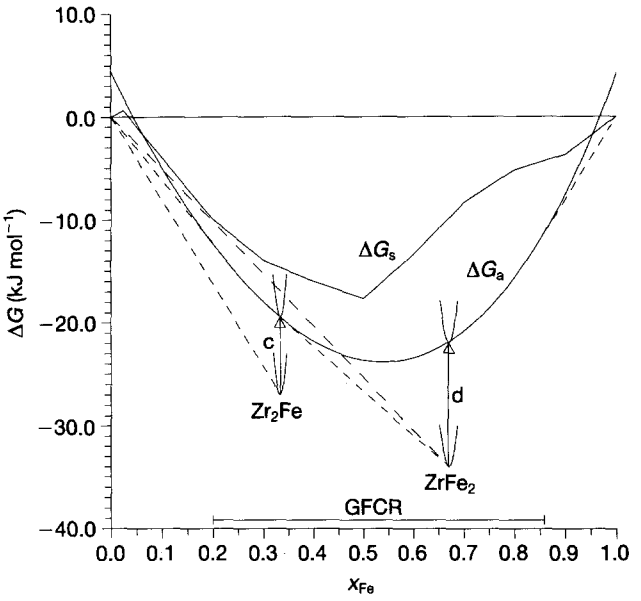


*Figure 1* Metastable free-energy diagram of the Zr–Fe alloy at $T$ = 580 K, showing the free energies of formation of the different phases as functions of the iron atomic fraction. Those phases are: s, solid solution (which is hcp for $x_{Fe} < 0.025$ and bcc for $x_{Fe} > 0.025$); a, amorphous alloy. Common tangents to the free-energy curves of several phases have been drawn (dashed lines). Arrows c and d indicate the effect of energy accumulation in the particles discussed in the text. The region labelled GFCR indicates the predicted glass-forming composition range assuming that the crystallization of intermetallic compounds can be kinetically by-passed.

## 3. Application of the free-energy diagram to discuss irradiation induced amorphization and dissolution of intermetallic particles in Zircaloy

Because our discussion of the behaviour of ternary intermetallic particles in Zircaloy under irradiation is based on a restricted analysis of the "model" system Zr– Fe, let us, as a previous step, check our method by briefly discussing the amorphization range of this binary alloy.

The calculated free energies of the Zr–Fe amorphous alloy, $\Delta G_a$, solid solutions, $\Delta G_s$, and of the $Zr_2Fe$ and $ZrFe_2$ intermetallic compounds, have been plotted in Fig. 1. The calculation has been performed at a temperature $T$ = 580 K. The curves for $Zr_2Fe$ and $ZrFe_2$ are schematic. Only the points corresponding to perfect stoichiometry are actually given by Miedema's model [22], and the curves just indicate that the free energy rises sharply when the composition deviates from the stoichiometric one. The free energy plotted for the metastable solid solution phase is the lower envelope of the $(\Delta G_s)_{\sigma=hcp}$ and $(\Delta G_s)_{\sigma=bcc}$ curves [19, 20]. The solid-solution phase is hcp for concentrations very rich in zirconium, that is, for $x_{Fe} < 0.025$, and bcc for other concentrations ($x_{Fe} > 0.025$). For the solid solutions, as well as for the amorphous alloy, we have taken $\gamma = 0$ in Equation 3, which assumes the absence of chemical short-range order in both phases. This leads to results consistent with the negligible solid solubilities of zirconium in bcc-Fe and iron in hcp-Zr, and with the fact that the equilibrium phase diagram below 1000 K is dominated by the presence of intermetallic compounds [28, 30, 31]. Two of those compounds, $Zr_2Fe$ and $ZrFe_2$, have been included in Fig. 1. The other two, $Zr_3Fe$ and $Zr_6Fe_{23}$, have not been plotted because those are not relevant for our discussion in this paper.

The predicted glass-forming composition range (GFCR) is indicated in Fig. 1. A comparison of $\Delta G_s$ and $\Delta G_a$ shows that $\Delta G_a$ is below $\Delta G_s$ over almost all the concentration range. The limits of the GFCR have been obtained by calculating the metastable equilibrium between the amorphous phase and the two pure metals through the common-tangent construction. If we assume that the formation of intermetallic compounds can be kinetically by-passed, then the predicted GFCR is rather broad ($0.2 \leqslant x_{Fe} \leqslant 0.86$). This extended range agrees quite well with the experimental one obtained by Krebs [32] by co-sputtering on silicon substrates at $T$ = 623 K. Amorphous films were obtained by this author over the whole composition range studied, $0.20 \leqslant x_{Fe} \leqslant 0.93$.

To explain the phenomenology concerning the stability of ternary intermetallic particles in Zircaloy under irradiation by particle beams, we will use, as a reference, the binary "model" system Zr–Fe. This

seems to be a reasonable approximation considering first that chromium, iron and nickel behave rather similarly as solutes in zirconium [33], and second that a relevant part of the behaviour to be explained is related precisely to adjustments of the iron concentration in the intermetallic particles and in the Zr(α), h c p matrix. We will not consider the detailed effect of different kinds of radiation beams on the stability of the intermetallic particles, as all of them are able to produce, even at small doses, amorphization of the intermetallic particles. The differences observed for the different kinds of radiation beams can be related to differences in damage morphology and displacement efficiency, and to the ability of the different irradiated phases to recover from irradiation damage.

At low temperatures, where atomic diffusion is slow, the low rate of defect recombination and the difficulty in adjusting compositions up to long distances favours the accumulation of energy, homogeneously, in the bulk of both kinds of precipitate particles ($Zr_2$(Ni, Fe) and Zr(Cr, Fe)$_2$) until these become unstable with respect to the metastable amorphous phase. The build-up of complexes (coupled interstitial–vacancy pairs) [2] could be a suitable mechanism of energy accumulation. This effect can be taken into account by raising the free-energy curves of the intermetallics relative to the free-energy curve of the amorphous phase [34]; this is represented by arrows c and d in Fig. 1. Once the free energy of the particle is higher than that of the amorphous phase, the whole volume of the particle will be able to transform spontaneously into the amorphous phase. This process does not involve adjustments of composition in the volume of the particle. From the Miedema model, the free-energy change required for the amorphization of $Zr_2Fe$ is $\sim 8\,kJ\,mol^{-1}$ (arrow c in Fig. 1). This free energy is of the same order of magnitude, although greater, than the free energy ($\sim 6.2\,kJ\,mol^{-1}$) calculated by Motta *et al.* [8] for the amorphization of $Zr_2$(Ni, Fe) particles under irradiation, assuming a mechanism of accumulation of simple point defects and lattice disordering. At low temperatures, particle dissolution can also take place [15]. We suggest that irradiation-enhanced solubility in the zirconium matrix is a plausible mechanism for particle dissolution. Irradiation can produce many defects, mainly vacancies and vacancy–interstitial pairs, in the zirconium matrix. These vacancies provide sites to which the atoms of the irradiated precipitate can migrate. The very low solubility in Zr(α) can be increased by this non-equilibrium process, leading to dissolution of the intermetallic particles. Evidently the relevance of this effect is limited by the slow low-temperature diffusivity.

In the intermediate temperature range, diffusion is faster than at low temperatures (also defect recombination in the particle is more efficient) and processes involving adjustments of composition become more significant. Consequently, the capacity to store energy in the intermetallic particles is progressively lowered and the dissolution of both kinds of particles becomes increasingly relevant. Nevertheless, at this point, different behaviours have been observed. While $Zr_2$(Ni, Fe) preferently dissolves, Zr(Cr, Fe)$_2$ is still able to amorphize under neutron and heavy-ion irradiation. The last process begins with the formation of an amorphous layer of composition around 33 at % (Fe + Cr) at the interface between the Zr(α) matrix and the Zr(Fe, Cr)$_2$ intermetallic particles [11] (notice that the concentration of Fe + Cr in the amorphous layer is lower than in the intermetallic). Afterwards, the amorphous layer advances into the particle. The limiting composition, $x_{Fe} \sim 0.2$, for equilibrium between the amorphous alloy and the zirconium matrix in Fig. 1 coincides with that observed by Yang [11] after the particle is completely amorphized. Evidently, for the reasons given above (low capacity to store energy in the particles), a mechanism for amorphization similar to that represented by arrow d in Fig. 1 is not possible in this range of temperature. But, in Fig. 1 we observe that the curve representing the free energy of the amorphous phase is, for $x_{Fe}$ smaller than 0.45, below the straight line joining the free-energy curves of Zr(α) and the $ZrFe_2$ intermetallic (this straight line represents the metastable equilibrium between the two crystalline phases). The relative position between those two lines then shows that there is a driving force for the nucleation of the amorphous phase. Fig. 1 also shows that simultaneous local metastable equilibrium conditions can be sustained at the respective interfaces Zr(α)–amorphous phase and $ZrFe_2$–amorphous phase during the growth of this amorphous layer (notice the common tangents between Zr(α) and the amorphous phase, and between the amorphous phase and $ZrFe_2$) and that the amorphous alloys are depleted in iron compared to the original composition in the intermetallic particle. However, similar conditions cannot be met for the nucleation of an amorphous phase between the zirconium matrix and $Zr_2Fe$. In this case, the mechanism of radiation-enhanced solubility described above can explain the dissolution of this particle in the zirconium matrix.

Once the amorphous layer nucleates at the interface between Zr(Cr, Fe)$_2$ and the Zr(α) matrix, it can advance into the particle, probably driven by ion mixing, to relax the free energy of the whole system. Interdiffusion of zirconium and iron (and chromium) adjusts the compositions of the phases to their local metastable equilibrium values.

Finally, amorphization of the particles has not been obtained under irradiation at high temperatures. Instead, dissolution of the particles with and without reprecipitation is the effect observed [5, 8, 10, 12, 15]. Both the dissolution and reprecipitation can be explained by the same mechanisms operating at intermediate temperatures, namely irradiation-enhanced solubility combined with a high atomic mobility, which can lead first to the dissolution of the particle, producing metastable supersaturated solid solutions and, later, to reprecipitation of the original intermetallic particles from the supersaturated solution. However, a new constraint should exist to prevent the formation of amorphous alloys from Zr(Cr, Fe)$_2$. A plausible one is that at high temperatures the system is probably above the glass temperature of the alloy (which to the best of our knowledge has not been measured yet) and amorphous phases cannot form.

## 4. Conclusion

Pursuing a previous analysis by Motta and Lemaignan [13], we have calculated the free-energy diagram of the reference system Zr–Fe and have considered some aspects of its modification by irradiation. With this simple approach the difference of amorphization behaviour between $Zr_2(Ni, Fe)$ and $Zr(Cr, Fe)_2$ intermetallic particles, which are present as precipitates in zirconium-based alloys of interest for the nuclear industry, is qualitatively understood.


## Acknowledgements

The authors thank E. Forlerer for the fruitful discussions maintained, and H. Tendler for his assistance in the computational task. This work was supported by the Spanish Ministry of Education and Science's Programme for Scientific Cooperation with Iberoamérica, the DGICYT (Project PB92-0645-CO3) and the Xunta de Galicia (Project XUGA 20602B92).


## References


1. W. L. JOHNSON, *Progr. Mater. Sci.* **30** (1986) 81.
2. D. F. PEDRAZA, *Metall. Trans.* **21A** (1990) 1809.
3. P. CHEMELLE, D. B. KNORR, J. B. VAN DER SANDE and R. M. PELLOX, *J. Nucl. Mater.* **113** (1983) 58.
4. T. O. MALAKHOVA and Z. M. ALEKSEYEVA, *J. Less-Common Metals* **81** (1982) 293.
5. J. B. VAN DER SANDE and A. L. B EMENT, *J. Nucl. Mater.* **52** (1974) 115.
6. M. GRIFFITHS, R. GILBERT and G. J. C. CARPENTER, *ibid.* **150** (1987) 53.
7. F. LEFEBVRE and C. LEMAIGNAN, *ibid.* **171** (1990) 223.
8. A. T. MOTTA, D. R. OLANDER and A. J. MACHIELS, ASTM-STP 1046 (American Society for Testing and Materials, Philadelphia, PA, 1989) p. 457.
9. R. W. GILBERT, M. GRIFFITHS and G. J. C. CARPENTER, *J. Nucl. Mater.* **135** (1985) 265.
10. W. J. S. YANG, R. P. TUCKER, B. CHENG and R. B. ADAMSON, *ibid.* **138** (1986) 185.
11. W. J. S. YANG, *ibid.* **158** (1988) 71.
12. F. GARZAROLLI, P. DEWES, G. MAUSNER and H. H. BASSO, in "Zirconium in the Nuclear Industry", 8th International Symposium ASTM-STP 1023 (American Society for Testing and Materials, Philadelphia, PA, 1989) p. 641.
13. A. T. MOTTA and C. LEMAIGNAN, *J. Nucl. Mater.* **195** (1992) 277.
14. Y. ETOH and S. SHIMADA, *ibid.* **200** (1993) 59.
15. R. A. HERRING and D. O. NORTHWOOD, *ibid.* **159** (1985) 386.
16. A. K. NIESSEN, F. R. DE BOER, R. BOOM, P. F. DE CHÂTEL, W. C. M. MATTENS and A. R. MIEDEMA, *Calphad* **7** (1983) 51.
17. A. R. MIEDEMA and A. K. NIESSEN, *ibid.* **7** (1983) 27.
18. A. K. NIESSEN and A. K. MIEDEMA, *Ber. Bunsenges. Phys. Chem.* **87** (1983) 717.
19. P. I. LOEFF, A. W. WEEBER and A. R. MIEDEMA, *J. Less-Common Metals* **140** (1988) 299.
20. A. R. MIEDEMA and A. K. NIESSEN, *Trans. Jpn Inst. Metals* **29** (1988) 209.
21. J. G. VAN DER KOLK, A. R. MIEDEMA and A. K. NIESSEN, *J. Less-Common Metals* **145** (1988) 1.
22. F. R. de BOER, R. BOOM, W. C. M. MATTENS, A. R. MIEDEMA and A. K. NIESSEN, "Cohesion in Metals. Transition Metal Alloys" (North-Holland, Amsterdam, 1988).
23. A. K. NIESSEN, A. R. MIEDEMA, F. R. de BOER and R. BOOM, *Physica* **B151** (1988) 401.
24. J. M. LÓPEZ, J. A. ALONSO and L. J. GALLEGO, *Phys. Rev.* **B36** (1987) 3716.
25. J. D. ESHELBY, *Solid State Phys.* **3** (1956) 79.
26. H. M. FERNANDEZ, Thesis, University of Santiago de Compostela, Spain (1993).
27. K. A. GSCHNEIDNER Jr, *Solid State Phys.* **16** (1964) 275.
28. D. ARIAS and J. P. ABRIATA, *Bull. Alloy Phase Diag.* **9** (1988) 597.
29. L. KAUFMAN and H. BERNSTEIN, "Computer Calculation of Phase Diagrams" (Academic Press, New York, London, 1970).
30. K. BHANUMURTHY and G. B. KALE, *Scripta Metall. Mater.* **28** (1993) 753.
31. H. OKAMOTO, *J. Phase Equil.* **14** (1993) 652.
32. H. U. KREBS, *J. Less-Common Metals* **140** (1988) 17.
33. R. TENDLER and J. P. ABRIATA, *J. Nucl. Mater.* **150** (1987) 251.
34. K.-Y. LIOU and P. WILKES, *ibid.* **87** (1979) 317.



*Received 28 April*
*and accepted 7 June 1994*